

Synergistic Reinforcing Influence of SiC, Al₂O₃, and CdS on Advanced Tribomechanical Properties of Aluminum Composites

Sachin S. Pande^{a,*} , R.G. Tikotkar^b , J. Balaji^c , Syed Sameer Hussain^d

^aDepartment of Mechanical Engineering, SECAB Institute of Engineering and Technology, VTU, Belgaum, Karnataka, India,

^bDepartment of Mechanical Engineering, BLDEA'S Engineering College, VTU, Belgaum, Karnataka, India,

^cDepartment of Mechanical Engineering, Dr Ambedkar Institute of Technology, VTU, Belgaum, Karnataka, India,

^dDepartment of Mechanical Engineering, SECAB Institute of Engineering and Technology, VTU, Belgaum, Karnataka, India.

Keywords:

Al6063 alloy
Mechanical properties
Wear resistance
Metal matrix composites
Nano-composites
SiC/ Al₂O₃/ CdS

ABSTRACT

This study utilized the stir casting method to examine the mechanical and tribological properties of Al6063 alloy nano-composites reinforced with varying volume fractions of Al₂O₃/SiC (2.5%, 5.0%, 7.5%, and 10%) and CdS (0.5%, 1.0%, 1.5%, and 2.0%). The investigation into the influence of filler content on mechanical properties revealed that the Al6063 alloy composites exhibited an increasing trend in tensile strength (241 MPa), hardness (72 BHN), and compression strength (325 MPa) compared to pure Al6063 alloy. However, as the filler content increased, the impact strength decreased to 26 KJ/m². Microstructural analysis, performed using advanced techniques such as scanning electron microscopy (SEM), provided a detailed examination of the worn surfaces. Tribological properties were assessed using the pin-on-disc method, measuring the coefficient of friction (COF) and specific wear rate (SWR) under varying conditions: loads of 5 N, 7.5 N, and 10 N; sliding distances of 1000 m, 2000 m, and 3000 m; rotational speed of 400 rpm; and sliding velocity of 0.5 m/s. At the highest load of 10 N and a sliding distance of 3000 m, the results showed a decreasing trend in SWR and COF, with values of $0.20 \times 10^{-4} \text{ mm}^3/\text{N-m}$ and 0.12, respectively.

* Corresponding author:

Sachin S. Pande
E-mail:
sachinpandeybijapur@gmail.com

Received: 22 August 2024

Revised: 6 October 2024

Accepted: 21 December 2024



© 2025 Published by Faculty of Engineering

1. INTRODUCTION

The continuous pursuit of innovative strategies to improve the performance of engineered materials remains a key focus in materials science and engineering. This effort aims to unravel the complex interactions

between reinforcing agents and the aluminum matrix, ultimately identifying the mechanisms responsible for the enhanced wear resistance observed. Metal Matrix Composites (MMCs) have developed as a critical subject in the material sciences, attracting both researchers and practitioners. The motivation behind this

study lies in the quest for tailoring the properties of hybrid materials to augment sliding wear resistance across diverse engineering applications. This study seeks to investigate the tribological behavior and microstructural characteristics of aluminum composites under different sliding conditions through detailed experimental analysis [1]. This field primarily involves the combination of man-made elements, resulting in composite constructions with two or more distinct phases smoothly bonded together. The matrix material is the foundational component in this composite design, and it houses materials with lower densities such as aluminium, titanium, steel, and so on. This intentional mixing of distinct phases produces materials with increased capabilities, pushing the boundaries of traditional material science and offering up new options for innovation [2]. Moreover, this research transcends the confines of the laboratory to explore the real-world implications of these tribological advancements. The spotlight is placed on the potential of these synergistically reinforced aluminum composites to revolutionize the landscape of wear-resistant materials [3]. The findings of this study promise to not only advance our understanding of the complex interplay between reinforcing agents and matrix but also pave the way for the development of advanced materials with superior tribological performance [4-7]. The evaluate concludes that the adding up of TiB_2 substantially improve the largely accomplished of aluminum alloys, in particular in terms of mechanical power and wear resistance. This makes TiB_2 a promising reinforcement material for developing superior aluminum-primarily based composites [8]. Aluminum metal matrix composites (AMMCs) gift promising future potentialities with ongoing advancements of their mechanical and thermal characteristics, making them increasingly feasible for excessive-performance applications [9]. In all of the foregoing procedures, the dimensions of the reinforcing powder ranges from microns to nano. Over the past ten years, advances in in-situ manufacturing technology have been made for the production of metallic and ceramic composites, with a particular emphasis on deciphering tribological breakthroughs [10-13]. Stir-casting are

utilized to make the aluminium matrix with Al_2O_3 (5 and 8 wt%), wear rate increases as normal load increases; however composite wear rate reduces as sliding distance increases with sliding velocity [14]. The Nanoclay is utilized as filler with Al6061, which increases mechanical qualities and has low wear resistance when compared to pristine Al6061. Similarly, the COF also decreases when the load increase [15]. The composite with Al and xGnP (0 to 5 wt %) is manufactured using the stir casting method. The composites improve wear resistance as the filler wt% increases up to 5 wt% but drop hardness beyond 1% of xGnP [16]. The aluminum metal matrix with filler Si and SiCp, tribological analysis revealed that as applied-load enhanced, wear rate and coefficient -of-friction diminish [17]. Wear particles from friction tests on standard disc brake materials are often larger and irregularly shaped, whereas those from unconventional materials, such as composites, are smaller, more uniform, and may contain complex phases due to varying reinforcing. These factors determine wear rate, thermal stability, and overall brake performance [18]. Researchers have spent decades studying the friction, and the wear behavior of motor vehicle braking equipment, with the goal of maximizing performance, durability, and safety under a variety of operating circumstances [19-23]. Although gray-cast-iron has traditionally been the chosen stuff for brake-drums and the disks, brake shoe, and pad materials continually shift into the more sophisticated compositions to improve performance, durability, and environmental sustainability [24]. The investigator studied waste aluminium with SAC and CDPF (1.25 to 6.25 V %) using the stir cast process. Mechanical strength improves significantly, while coefficient-of-friction and the wear-rate decrease significantly [25]. The wear resistance of the Al- Al_2O_3 combination was tested using the pin-on-disc method, and it was discovered that the composite increased in hardness when compared to neat Al alloy. Adding 1% V_2O_5 improves the wear-rate and efficiency of the friction [26]. Employing the situ process, there was a gradual decrease in COF and wear resistance as the TiB_2 filler with Al6063 matrix increased [27]. Investigation of the Al6351 matrix with the hybrid filler Gr and SiC at appropriate weight and determined the

reduction in ductility by SiC and the decrease in elongation owing to the presence of Gr [28]. Wear tests were conducted on Al7075 with Gr and Al₂O₃. By holding Gr at 5 wt% and varying the Al₂O₃, the outcome suggested the inclusion of graphite improves wear-resistance [29]. Wear tests on MMC of Al/Zn5%/SiC 10% revealed that COF decreased as load increased, and that the addition of SiC increased tensile, and hardness over neat Al6061 alloy [30]. The tribological behaviour of AA7075-TiC composites generated by powder metallurgy shows improved wear resistance and reduced friction due to the synergistic effects of the hard TiC particles within the Al matrix [31]. The inclusion of titanium di-boride ceramic particles to Cu-10 wt.% Al6061 alloy composites manufactured via powder metallurgy produces a homogeneous dispersion of ceramic particles and has a hardening effect, it significantly increases mechanical strength and wear resistance [32]. The addition of graphite to Al6061/SiC hybrid composites improves their tribological properties by reducing friction and wear, while also marginally enhancing mechanical qualities due to the solid lubricant effect of graphite [33]. Demonstrate that incorporating rice-husk-ash and alumina into Al/Mg/Si alloy composites increases both corrosion resistance and wear behaviour, providing a long-term solution for improving material performance [34]. Powder metallurgy was used to manufacture an Al matrix with fillers such as micro SiC (10wt %) and nano SiC (0 to 7 wt%). It was found that the wear resistance, hardness, and nano SiC (5 wt %) composition performed better than the other compositions [35]. The mechanical/tribological features of Al alloy matrix with micro SiC/nano-ZrO₂ filler were studied, and it was revealed that the wear-rate of the composites decreases as the ZrO₂ concentration raised [36]. The wear resistance and micro-hardness of aluminum-based hybrid composites synthesized via powder metallurgy are affected by changes in the concentration of rutile (TiO₂). The investigator finds significant increases in material attributes [37]. Researcher focuses on advanced techniques such as powder metallurgy, spark plasma sintering, and additive manufacturing (e.g., 3D printing). These methods enable precise control over

material composition and microstructure, minimizing material wastage while achieving complex geometries [38]. The results indicate that raising the melt temperature and using a gating system with a higher heat transfer rate improve the ultimate tensile strength (UTS) of pure aluminum by 7%. Additionally, adding 2 wt% Al-5Ti-1B grain refiner in bar form to the overheated melt doubles the UTS, while introducing the same grain refiner in micro-powder form achieves a 32% increase in UTS compared to samples without the grain refiner [39]. The dissolution of ceramic particles into the aluminum matrix enhances the bonding strength between the particles and the matrix. Incorporating reinforcement particles into Al alloy matrix significantly improves specific strength, stiffness, wear resistance, fatigue, and creep properties compared to conventional engineering materials [40-42].

2. MATERIALS & METHODS

2.1 Material

The detailed composition of the base material, Al6063, is presented in Table 1. The reinforcement materials used in this study include 25 nano-sized particles of silicon carbide (SiC), aluminum oxide (Al₂O₃), and cadmium sulfide (CdS). These nano-particles were procured from Biomall, located in Andheri East, Mumbai, India. The base material, Al6063, was sourced from 4MANN Industries Private Ltd, also situated in Andheri East, Mumbai, India. These materials were utilized to develop the hybrid metal matrix composites, with the nano-sized fillers serving as the primary reinforcing agents to enhance the mechanical and tribological properties of the Al6063 matrix.

Table1. Elemental composition of Al6063 [43].

Material	Fe	Mn	Zn	Mg	Ti
Element (%)	0.35	0.1	0.1	0.45-0.9	0.1
Material	Cu	Cr	Si	Al	
Element (%)	0.1	0.1	0.2 - 0.6	Balance	

2.2 Method

We use the stir casting technique in this work because it provides an easy-to-use and affordable method for creating composites

with a hybrid aluminium metal matrix. First, the base material, Al-6063 powder, and the selected fillers, SiC, Al₂O₃, and CdS, are precisely weighed. High-energy ball milling is used to thoroughly mix the powder and guarantee that the fillers are evenly dispersed throughout the aluminium matrix. In a furnace, the Al6063 alloy is melted at a temperature of approximately 700°C to 750°C. To release any trapped gases, the molten metal needs to be degassed. This is often accomplished with the use of an argon or nitrogen degassing agent. Before adding SiC, Al₂O₃, and CdS particles to the molten aluminium, they should be warmed to a temperature of around 200°C to 300°C. Preheating improve the wet ability of the nano material by the molten aluminium and aids in the removal of moisture and other impurities. After adding a mechanical stirrer to the molten aluminium, the mixture is stirred for ten minutes at a speed of about 300 rpm. To achieve uniform distribution, the warmed SiC, Al₂O₃, and CdS particles are injected progressively to the vortex formed by the stirring process. Usually, the stirring temperature is kept constant. The melted metal is combined with the reinforcing particles and then poured into heated moulds to take on the required shape. To prevent rapid cooling and thermal stress within the cast material, the molds are preheated to a temperature ranging from 200°C to 300°C. Preheating ensures that the molten metal does not cool too quickly upon contact with the mold, thereby reducing the risk of defects like cracks or distortions caused by thermal shock. The molten composite, which now contains the uniformly distributed reinforcing particles, is poured into the preheated molds. This process is done carefully to avoid splashing or trapping air bubbles that could lead to porosity in the final product.

The sample composition is manufactured according to the table 2.

Table2. Broad spectrum of Hybrid MMCs.

Specimen	Combination Volume (%)
A1	Al6063
A2	Al6063+2.5%SiC+2.5%Al ₂ O ₃ +0.5%CdS
A3	Al6063+5%SiC+5%Al ₂ O ₃ +1.0%CdS
A4	Al6063+7.5%SiC+7.5%Al ₂ O ₃ +1.5%CdS
A5	Al6063+10%SiC+10%Al ₂ O ₃ +2.0%CdS

2.3 Analysis and characterization of MMC composites

2.3.1 Tensile strength

A tensile test is a fundamental mechanical test in which a material is subjected to an applied uniaxial tensile force using a Universal Testing Machine (UTM-TUE-C-200 computerized) until it fractures. The specimen should be standardized in accordance with ASTM E8/E8M, which is frequently used for metals. Typically, the specimen (Fig. 1) resembles a dog bone and has a smaller centre cross-sectional area ($d=10\text{mm}$, $d_0=6\text{mm}$ $l=30\text{mm}$, $l_0=55\text{ mm}$). Insert the specimen into the tensile testing apparatus's grips. To prevent bending pressures, the alignment must be flawless. Make sure the grips don't slide or fail too soon, holding the specimen firmly. Although the strain rate can change, for metals like Al6063, it is typically about 0.1 mm/mm per minute utilizing the load cell.



Fig. 1. Tensile specimen.

2.3.2 Compression strength

To guarantee uniform distribution of the compressive load during a compression test, the Al6063 specimen is positioned vertically between two platens of the compression testing apparatus. The apparatus then measures the applied load and the resulting deformation while applying progressively more load until the specimen (Fig. 2) cracks or deforms. The dimension of the specimen is diameter 10mm with length 20mm.



Fig. 2. Compression specimen.

2.3.3 Hardness

The hardness test measures the resistance of a material to deformation, typically by indentation. Here's a general procedure for conducting a hardness test, specifically using common methods like Brinell hardness on Al6063 alloy. Ensure the surface of the Al6063 specimen (Fig. 3) is smooth, clean, and free of any contaminants. Polishing may be necessary to achieve a mirror-like finish for accurate results. Suitable for materials with a coarse or uneven structure, a 10 mm steel or tungsten carbide ball indenter is typically used with a load of 500 kgf for aluminum. Lower the indenter onto the specimen's surface and apply the load gradually. The load is held for a specified time (dwell time), usually 10-15 seconds. For accurate results, perform multiple indentations at different locations on the specimen and calculate the average hardness value.



Fig. 3. Hardness specimen.

2.3.4 Impact strength

The impact test determines the material's toughness—its ability to resist fracture and absorb energy in the case of a destructive impact. For Charpy or Izod testing, adhere to the ASTM E23 standard. The standard measurements are 55x10 x10 mm, with a V-notch 2 mm deep in the middle as shown in Fig. 4. Usually, the apparatus consists of a swinging pendulum hammer that strikes the specimen in a vertical position for an Izod test or a horizontal setup for a Charpy test. Place the specimen vertically so that the pendulum faces the notch. Using the energy scale as a guide, raise the pendulum to the desired height. The potential energy that the pendulum will possess upon striking the specimen is correlated with this height. The energy that the specimen absorbs during

fracture will be recorded by the machine. Recall that the energy absorbed is typically expressed in joules. The material's toughness is indicated by this value.

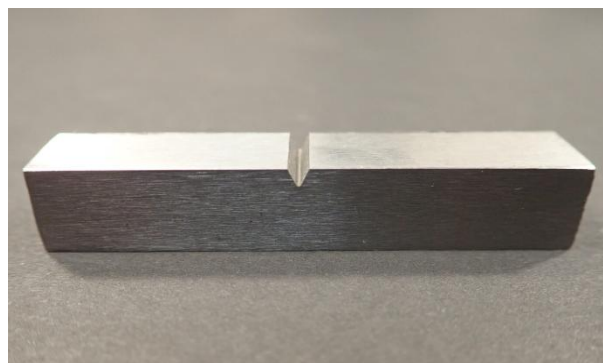


Fig. 4. Impact specimen.

2.3.5 Wear properties

A pin on disc (TR-20LEPHM) wear testing apparatus that complied with ASTM-G99 standard was used to evaluate the wear behaviour of the nano-composite samples under dry sliding conditions. The figure 5 depicts a pictorial image of the pin on disc configuration. Every experiment was carried out in ambient settings and at the temperature of the room. For the nano-composite test pins, a force applied of 5, 7.5, and 10 N was used. At 0.5 m/s, sliding distances of 1000, 2000, and 3000 m were investigated. The test pins were manufactured with a 10 mm in diameter and the length of 30 mm (Fig. 6). The disc surface had a diameter of 25 mm and served as the sliding route. Following each test, the weight loss of the pin was measured with an electronic balance. In tribology, the study of specific wear rate (SWR) and coefficient of friction (COF) are fundamental ideas.



Fig. 5. Wear Testing apparatus for experimentation.



Fig. 6. Wear test pin.

The SWR (k) is a metric that measures a material's wear performance under frictional conditions. It shows the amount of material worn away per unit (v) of distance moved (S) and applied stress (F). It measures the amount of material that wears off a surface. Usually, the precise wear rate is stated as follows.

$$k = \frac{V}{F \cdot S} \quad (1)$$

Where V = volume of worn material (m^3), F = Applied load (N), s = sliding distance (m)

The units of the specific wear rate are typically $\frac{m^3}{N \cdot m}$. A higher specific wear rate indicates that more material is worn away under given conditions, signifying poorer wear resistance.

2.3.6 Coefficient of friction

It's a number that represents the resistance between two surfaces when they are sliding against each other. It can be expressed as:

$$\mu = \frac{\text{Frictional force}}{\text{Normal force}} \quad (2)$$

The typical range for the coefficient of friction is from 0 (no-friction) to above 1 (high friction), while the exact value will depend on the materials and surface conditions.

2.3.7 Micro structure analysis

Microstructure analysis entails analyzing their internal structure at the microscopic level, scanning electron microscopy (SEM- Model-JEOL JSM-6480LV) are common methods used for this kind of investigation. Microstructure analysis provides insights into how processing conditions, heat treatments, and alloy compositions affect a material's mechanical

characteristics, wear resistance, and general behaviour by observing features such as grain size, phase distribution, inclusion content, and defect structures.

3. RESULTS AND DISCUSSIONS

3.1 Tensile-strength

The tensile strength of Al6063 and nano reinforcement containing 5.5, 11, 16.5, and 22 V% of SiC/Al₂O₃/CdS particles are illustrated in Fig. 7. Sample A2 showing a slightly higher value than the Al6063 alloy, it is a result of the SiC/Al₂O₃/CdS alloy's strong interface bonding with the Al6063 alloy matrix and its ability to tolerate applied load. The tensile strength keeps on increasing manner from sample A₂ to A₅ like 222 MPa to 241 MPa, which is almost 20% increase than Al6063 alloy. The nano reinforcements operate as the second phase in the matrix, limiting dislocation motion and resulting in an increase in the tensile strength of the nano metal matrix composite. It demonstrates a progressive increase in tensile strength with the addition of nano reinforcements, peaking at a maximum of 20%. These nano fillers restrict the mobility of molecule of matrix alloy so that the tensile strength improves. The addition of CdS typically reduces the matrix's tensile strength, but the SiC/Al₂O₃ reinforcement increases strength by shifting load from the Al6063 matrix to the SiC/Al₂O₃ fillers.

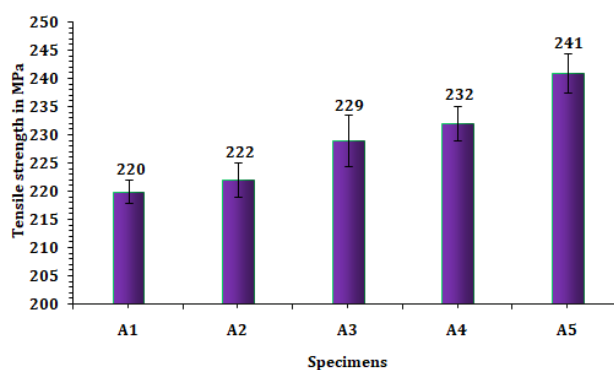


Fig. 7. Tensile strength of Al6063 MMC composite samples.

3.2 Compressive strength

The compressive strength of Al6063 metal alloy composites supplemented with nano particles varies from 220 to 325 MPa, as shown in Fig. 8. The Al6063 alloy has a compressive strength of 220 MPa. When 5.5 V% SiC/Al₂O₃/CdS

reinforcement is added, the composite's compressive strength increases by 12% to 250 MPa. Comparably, the strength of the composite improves from 250 to 325 MPa as the nano reinforcement increases compared to the Al6063 alloy. The nano composites' overall 33% gains in compressive strength are attributable to the inclusion of SiC and Al₂O₃, which also enhance the composites' capacity to withstand loads. The Al6063 alloy composites are made hard and void-free by these reinforcements, which indicates an increase in compressive strength. Samples A2 – A5 demonstrate an increase in compressive strength when compared to A1.

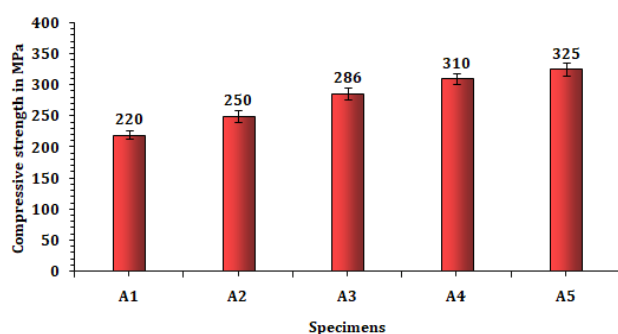


Fig. 8. Compressive strength of Al6063 MMC composite samples.

3.3 Hardness strength

The outcome of the hardness test on Al6063 alloy using nano composites containing 5.5, 13.5, 16.5, and 22 v% of nano of Al₂O₃, SiC, and CdS particles are shown in Fig 9. The sample A2 composites measures 50 BHN, whereas the Al6063 alloy's lowest hardness value is 42 BHN. These values continue to improve as the filler content increases. It has also been noted that the composition of A3 is 62 BHN hard and that of A5 is 72 BHN hard. All of the compositions exhibit greater hardness than the base Al6063 alloy because of the inclusion of SiC, Al₂O₃, and less CdS particles. Although it also increases brittleness, a greater amount of reinforcements results in a surface that is significantly harder. The trend in hardness indicates a direct correlation with the percentage of SiC, Al₂O₃, and CdS added to the Al6063 alloy. As the nano fillers addition increases, the hardness improves steadily. This is due to the ceramic particles' inherent hardness, which resists deformation and enhances the overall material strength

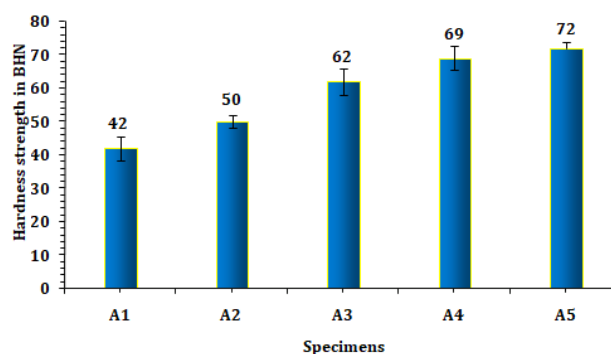


Fig. 9. Hardness strength of Al6063 MMC composite samples.

3.4 Impact strength

The impact values for the materials listed, each with varying compositions of Al6063 alloy and reinforcements, are influenced by the presence of Silicon-Carbide (SiC), Aluminum-Oxide (Al₂O₃), and Cadmium Sulfide (CdS) as shown in Fig 10. Pure Al6063 serves as the base alloy impact strength is 56 KJ/m² and typically has moderate impact resistance, characterized by a balance of ductility and strength. The introduction of small amounts of SiC and Al₂O₃ as reinforcements slightly increases hardness while still maintaining some ductility. CdS in a minor amount enhances particle bonding. Slightly lower than A1 46 KJ/m² due to increased brittleness from added ceramic particles. With a higher concentration of reinforcements, hardness improves, but the material becomes more brittle, reducing impact resistance 38 KJ/m² further lower than A2, indicating increased brittleness. A significant increase in reinforcement content further enhances hardness, but at the cost of substantial ductility, making the material even more brittle. Sample A4 are lower than A3, showing a further decline in impact strength 30 KJ/m². At this level, the material is highly reinforced, with exceptional hardness but drastically reduced ductility, leading to minimal impact resistance 26 KJ/m² which is sample A5. The general trend indicates that as the percentage of SiC, Al₂O₃, and CdS increases, the material becomes harder but more brittle, leads to a consistent decline in impact strength. The addition of ceramic reinforcements improves mechanical properties like hardness, but they compromise the material's ability to absorb energy during impact, making it more susceptible to fracture.

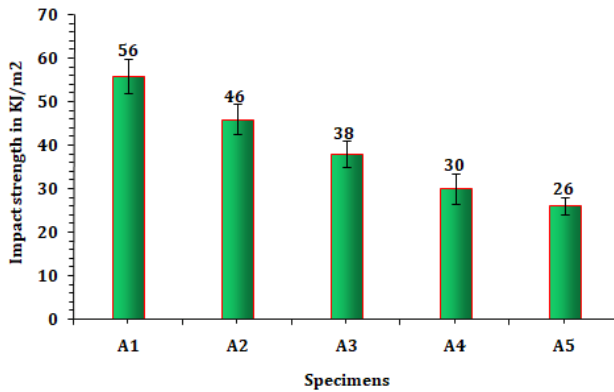


Fig. 10. Impact strength of Al6063 MMC composite samples.

3.5 Specific wear rate

Figure 11 (a-c) illustrate the variations of Specific wear rate with load of 5, 7.5 and 10 N for 1000, 2000, and 3000 m sliding distance, 0.5 m/s velocity for track radius 25 mm of various compositions of Al6063 alloy and Al6063/SiC/Al₂O₃/CdS nano composites. It is investigated that the load that was applied increased, while the SWR dropped because of the creation of mechanically mixed layer (MML) at high load. In all the compositions, an increase in v% of the nano materials (SiC/Al₂O₃/CdS) led to the decrease the wear rate due to increase in hardness of Al6063/SiC/Al₂O₃/CdS composites for the applied load. The hard nano SiC/Al₂O₃/CdS fillers on incorporating with Al6063 alloy makes good interfacing bonding, improves the strength and hardness of nano composites. These nano fillers operate as load carriers during sliding and safeguard the Al6063 alloy matrix from wearing out, resulting in increased wear resistance of nano-compositions. The wear rate decreases 1.2 to 1.6 %, on increasing the nano SiC/Al₂O₃/CdS fillers. The wear rate of Al6063/SiC/Al₂O₃/CdS at sliding distance 1000 m was higher than the 2000 and 3000 m for different applied load.

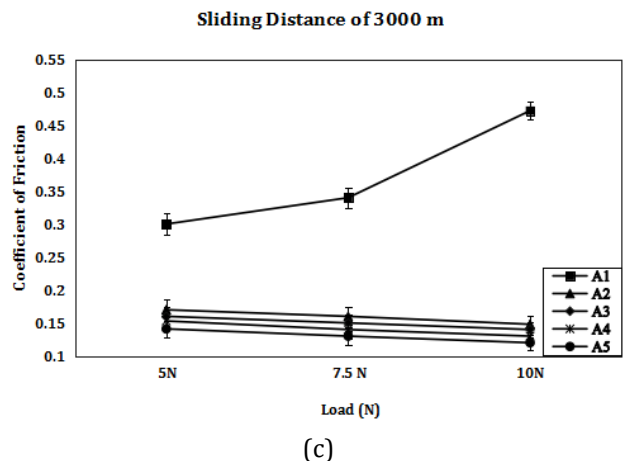
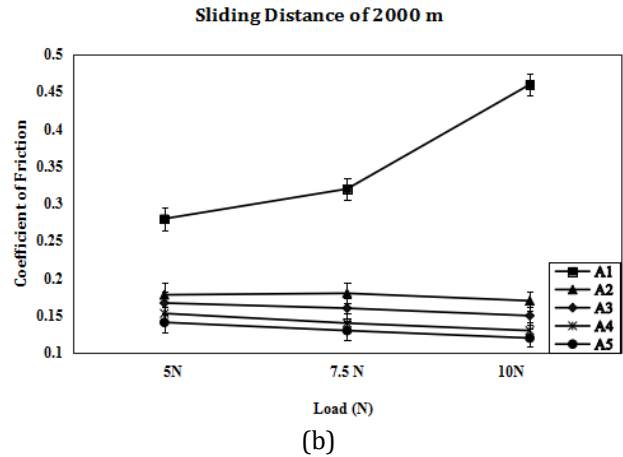
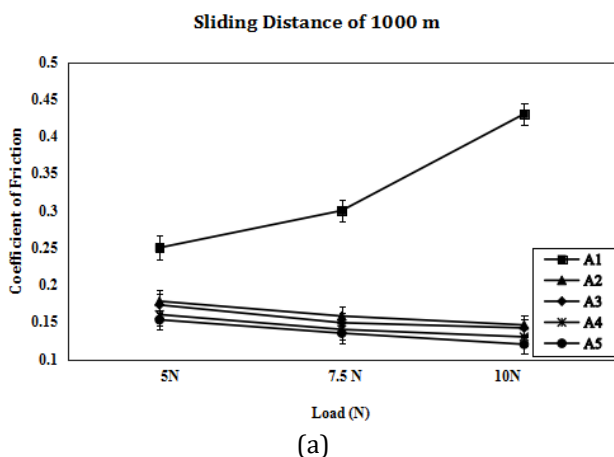


Fig. 11. SWR of nano metal matrix composites at (a) 1000m, (b) 2000m and (c) 3000m sliding distance under different loads.

The MML favors the SWR to decreases as the sliding distance increases. A1 does not show this beneficial trend, indicating it may either lack MML formation or have less effective wear protection under increasing loads. This analysis supports the idea that the formation of an MML can decrease the specific wear rate, particularly for materials like A2 to A5.

3.6 Co-efficient of friction

Figure 12 (a-c) shows that the variation of coefficient of friction with respect to load of 5, 7.5, and 10 N for track radius = 25 mm, sliding distance = 1000, 2000, and 3000 m and 0.5 m/s velocity with various composition of Al6063 alloy and Al6063/Al₂O₃/SiC/CdS nano composites. The nano composites sample from A2 to A5 are lower COF than the Al6063 alloy for applied different loads. The sample's COF decreases as the load increases because the Al₂O₃/SiC/CdS fillers incorporated in the Al6063 matrix reduce the surface contact

between the pin sample and rotating disc outcome in diminish frictional force which indicates the reduced COF. The sliding distances are not greatly affected to the COF of nano composites. The decrease in the friction of the Al6063/Al₂O₃/SiC/CdS reinforced composition because of increased hardness and MML formation reduce the plastic flow at the surface contact. For different loads, the friction values of various v% of Al₂O₃/SiC/CdS depict slightly varied. Figure 8 (a-c) implies that the COF of Al6063 = 0.47 at 7.5 N load and 3000 m sliding distance compare to the Al6063/Al₂O₃/SiC/CdS nano composition is 0.12. This implies the incorporation of nano particles reduce the friction of the nano-composites. The good interface between matrix and nano particles, uniform distribution, good bonding and less heat generation in between the surface contact. The increasing trend for A1's coefficient of friction suggests that it may not be suitable for high-load applications where low friction is desirable. A2, A3, A4, and A5 maintain lower friction, making them better choices for applications requiring efficient and stable performance under varying loads.

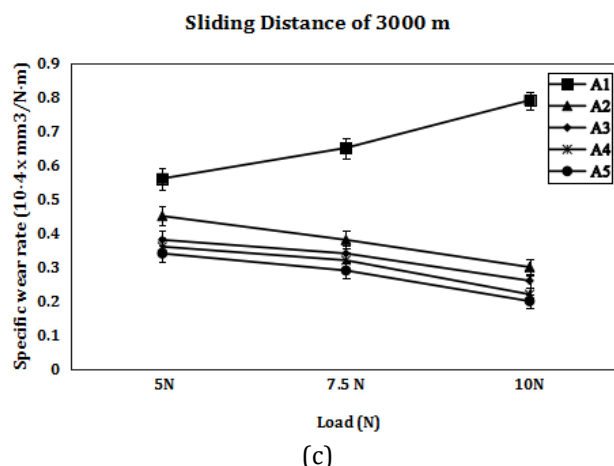
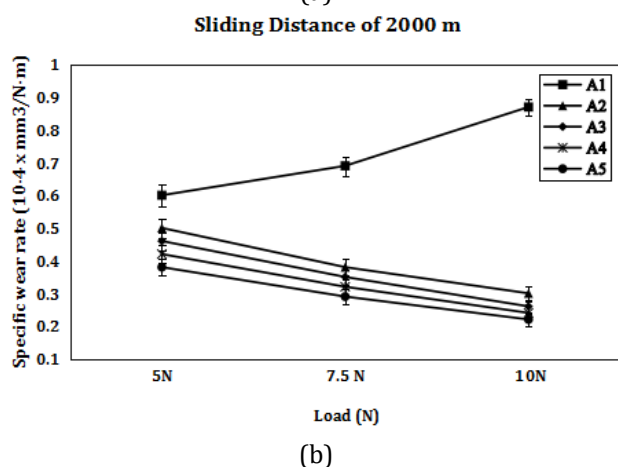
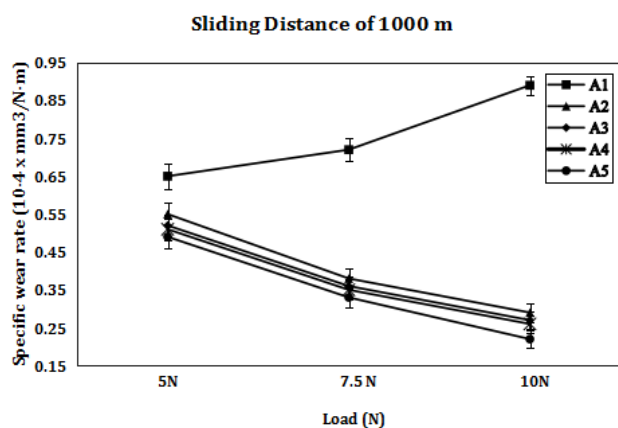


Fig. 12. COF of nano-metal matrix composites at (a) 1000m, (b) 2000m, (c) 3000m sliding distance under varying load.

3.7 Microstructure characterization

The Sem images of individual nano fillers and base metal matrix are depicted in figure 13 (a-d). The SEM micrograph depicts silicon carbide (SiC) particles with a spherical morphology and a range of particle sizes and Al₂O₃ (aluminum oxide or alumina) particles with an irregular and agglomerated morphology. The SEM micrograph illustrates a CdS (cadmium sulfide) material with a granular and agglomerated morphology. In unreinforced Al6063, defects such as micro-voids, pores, or shrinkage cavities might be visible.

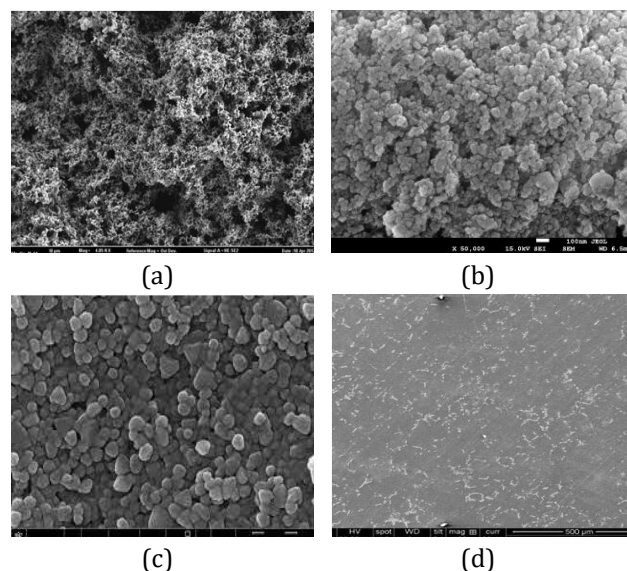


Fig. 13. SEM images of (a) SiC, (b) Al₂O₃, (c) CdS, (d) Al6063 alloy matrix.

The tensile fracture behavior of Al6063 alloys as shown in figure 14 a), with or without reinforcements, predominantly shows ductile

fracture features under SEM, such as dimples and void coalescence. However, the fracture morphology can be influenced by factors like microstructure, second-phase particles, and processing conditions. The tensile fracture behavior of Al6063 reinforced with fillers is significantly influenced by the type, distribution, and bonding of the reinforcement particles. Reinforcement tends to cause both ductile and brittle fracture features due to its hardness and stress-concentrating nature, dimples and void conditions as shown in figure 14 b).

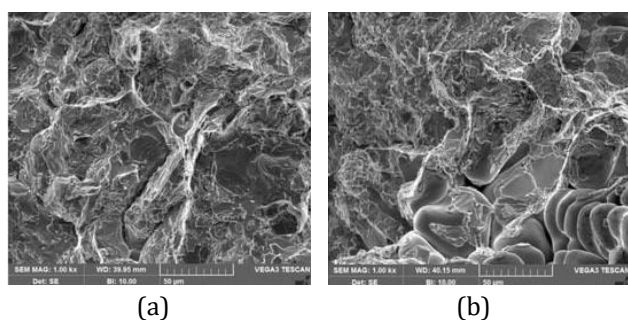


Fig. 14 Tensile fracture of (a) A1 sample, (b) A3 sample.

Under impact conditions, Al6063 typically exhibits ductile fracture with energy absorption through dimples and plastic deformation as shown in figure 15 a). Figure 15 b) shows the impact fracture behavior of Al6063 with reinforcement SiC, Al₂O₃, and CdS depends on the nature of the reinforcement and its interaction with the aluminum matrix. Reinforcement increases strength and toughness, offering a better balance between ductility and impact resistance.

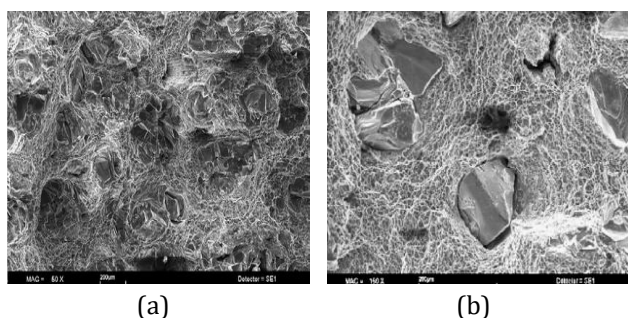


Fig. 15. Impact fracture of (a) A1 sample, (b) A3 sample.

The worn surface of Al6063 alloy matrix and Al6063/Al₂O₃/SiC/CdS nano composites pin run over the disc at load 10 N as depicted in below Figure 16 (a-d). SEM images display important information on wear mechanism of neat Al6063 alloy and nano composites. Figure 16(a-b) illustrates the furrows & scratches

caused by abrasive-wear that are visible on the deteriorated surface of Al6063 alloy (A1) at 10 N. Abrasive wear is believed to be a primary wear mechanism based on the patterns that have been found. Strong evidence of hard, abrasive particles scratching the surface is shown by the parallel furrows. Particles of detritus suggest a certain level of adhesive wear where material transfers and is then removed.

Figure 16 (c-d) depicts the SEM image of surface of worn of Al6063/Al₂O₃/SiC/CdS (A3) nano-composite at load 10 N notified that less deep grooves are evident of abrasive wear. It reveals shallow, parallel grooves that show signs of wear from abrasion. The presence of CdS functions as a lubricating layer on the deteriorated surface of the nano-composite, reducing the creation of grooves and less plastic deformation at the corners of the grooves. The worn surface of A3 nano-composite appears smooth, compared to A1 Al6063 alloy.

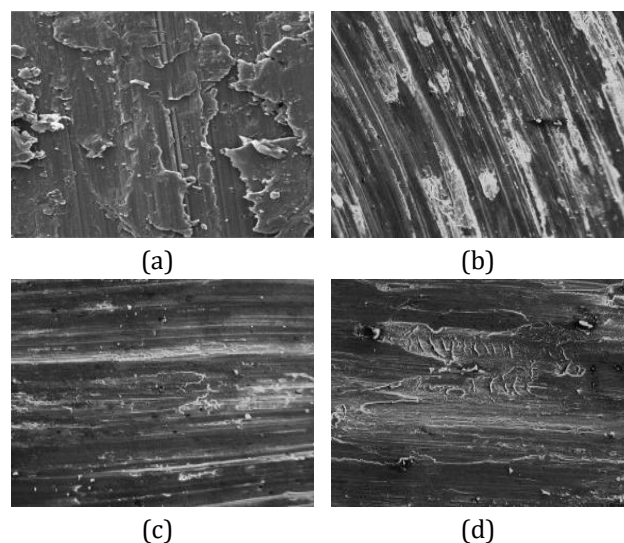


Fig. 16. Worn surface of nano-composite (10 N) a) & b) A1 sample and c) & d) A3 sample.

3.8 X-Ray diffraction (XRD)

The provided image shows an X-Ray Diffraction (XRD) pattern for a hybrid metal matrix composite consisting of Al6063 reinforced with 10% SiC, 10% Al₂O₃, and 2.0% CdS as shown in figure 17. The XRD peaks are plotted with intensity (a.u.) on the y-axis and 2θ (degrees) on the x-axis. The graph identifies characteristic peaks corresponding to the different phases present in the composite, namely Aluminum (Al), Silicon Carbide (SiC), Alumina (Al₂O₃), and

Cadmium Sulfide (CdS). Each phase is marked with specific symbols for easy differentiation. Prominent peaks appear at certain 2θ values, indicating the crystallographic planes of the reinforcing materials and the aluminum matrix. SiC introduces peaks characteristic of its hexagonal structure, Al_2O_3 reinforces the matrix with its corundum peaks, and CdS provides diffraction peaks.

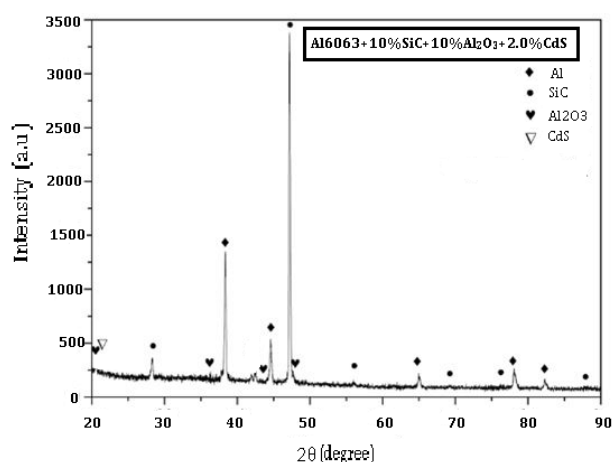


Fig. 17. XRD image for A5 sample.

4. CONCLUSIONS

In this present investigation, Al6063 nano composites with various v% of Al_2O_3 /SiC/CdS were manufactured using stir-casting method. The mechanical characterization like tensile, compressive, impact, hardness, and tribological characteristics of neat Al6063 alloy and Al6063/ Al_2O_3 /SiC/CdS nano-composites were investigated. Based on the experimental work, the following conclusions are portrayed.

- The tensile, compressive and hardness strength of Al6063/ Al_2O_3 /SiC/CdS nano-composites improved due to the presence of Al_2O_3 /SiC nano materials. But the impact strength of nano composites are drastically decreases because reinforce fillers are not able to absorb the energy of impact force.
- The addition of Al_2O_3 /SiC/CdS to Al6063 alloy strengthens wear resistance, which minimizes the SWR and COF of nano-composites for all sliding distances and loads.
- The inclusion of Al_2O_3 /SiC/CdS fillers and the building of a smooth CdS tribo-layer at the surface contact increase the wear resistance of nano-composites.

- In conclusion, it is determined that, in comparison to the A1 (Al6063 alloy), the A2-A5 nano-composites present better mechanical and tribological characteristics.

The industrial applications of these composites arise from their superior mechanical properties and excellent wear resistance, making them ideal for aerospace components like structural frames, brackets, and panels, as well as automotive parts such as engine blocks, pistons, brake rotors, and drive shafts due to their thermal stability, durability, and lightweight characteristics.

REFERENCES

- [1] K. Umanath, K. Palanikumar, and S. T. Selvamani, "Analysis of dry sliding wear behaviour of Al6061/SiC/ Al_2O_3 hybrid metal matrix composites," *Composites Part B Engineering*, vol. 53, pp. 159–168, Apr. 2013, doi: [10.1016/j.compositesb.2013.04.051](https://doi.org/10.1016/j.compositesb.2013.04.051).
- [2] S. T. Reddy, H. S. Manohar, and S. N. Anand, "Effect of carbon black nano-fillers on tribological properties of Al6061-Aluminium metal matrix composites," *Materials Today Proceedings*, vol. 20, pp. 202–207, Dec. 2019, doi: [10.1016/j.matpr.2019.11.045](https://doi.org/10.1016/j.matpr.2019.11.045).
- [3] P. K. Swain, K. D. Mohapatra, and P. K. Swain, "Synthesis and development of Al + SiCp nano composites and study of its machining processes," *Materials Today Proceedings*, vol. 33, pp. 5612–5616, Jan. 2020, doi: [10.1016/j.matpr.2020.03.714](https://doi.org/10.1016/j.matpr.2020.03.714).
- [4] J. Majhi, A. Mandal, S. K. Sahoo, S. C. Patnaik, B. Sarangi, and K. P. Jena, "Effect of pouring temperature on microstructure and mechanical properties in Al-16Si-2% Al_2O_3 hypereutectic alloys," *Materials Today Proceedings*, vol. 33, pp. 5539–5543, Jan. 2020, doi: [10.1016/j.matpr.2020.03.496](https://doi.org/10.1016/j.matpr.2020.03.496).
- [5] P. Suresh, K. Marimuthu, S. Ranganathan, and T. Rajmohan, "Optimization of machining parameters in turning of Al-SiC-Gr hybrid metal matrix composites using grey-fuzzy algorithm," *Transactions of Nonferrous Metals Society of China*, vol. 24, no. 9, pp. 2805–2814, Sep. 2014, doi: [10.1016/s1003-6326\(14\)63412-9](https://doi.org/10.1016/s1003-6326(14)63412-9).
- [6] N. S. S. Raju, G. S. Rao, and C. Samantra, "Wear behavioral assessment of Al-CSAp-MMCs using grey-fuzzy approach," *Measurement*, vol. 140, pp. 254–268, Apr. 2019, doi: [10.1016/j.measurement.2019.04.004](https://doi.org/10.1016/j.measurement.2019.04.004).

- [7] L. Yuan, J. Han, J. Liu, and Z. Jiang, "Mechanical properties and tribological behavior of aluminum matrix composites reinforced with in-situ AlB₂ particles," *Tribology International*, vol. 98, pp. 41–47, Feb. 2016, doi: [10.1016/j.triboint.2016.01.046](https://doi.org/10.1016/j.triboint.2016.01.046).
- [8] X. Wang, A. Jha, and R. Brydson, "In situ fabrication of Al₃Ti particle reinforced aluminium alloy metal-matrix composites," *Materials Science and Engineering A*, vol. 364, no. 1–2, pp. 339–345, Oct. 2003, doi: [10.1016/j.msea.2003.08.049](https://doi.org/10.1016/j.msea.2003.08.049).
- [9] B. Singh et al., "A future prospects and current scenario of aluminium metal matrix composites characteristics," *Alexandria Engineering Journal*, vol. 76, pp. 1–17, Jun. 2023, doi: [10.1016/j.aej.2023.06.028](https://doi.org/10.1016/j.aej.2023.06.028).
- [10] S. A. Farooq et al., "Effect of TiB₂ on the mechanical and tribological properties of marine grade Aluminum Alloy 5052: An experimental investigation," *Journal of Materials Research and Technology*, vol. 29, pp. 3749–3758, Feb. 2024, doi: [10.1016/j.jmrt.2024.02.106](https://doi.org/10.1016/j.jmrt.2024.02.106).
- [11] Y. Dou, Y. Liu, Y. Liu, Z. Xiong, and Q. Xia, "Friction and wear behaviors of B₄C/6061Al composite," *Materials & Design (1980-2015)*, vol. 60, pp. 669–677, Apr. 2014, doi: [10.1016/j.matdes.2014.04.016](https://doi.org/10.1016/j.matdes.2014.04.016).
- [12] J. Balaji, M. M. Nataraja, K. Sadashiva, and S. Supreeth, "Experimental and Computational Analysis of Thermal Characteristics of Polymer Resin Reinforced with Rice Husk and Aluminium Nitride Filler Composites," *Journal of the Institution of Engineers (India) Series D*, vol. 105, no. 1, pp. 313–321, Apr. 2023, doi: [10.1007/s40033-023-00480-z](https://doi.org/10.1007/s40033-023-00480-z).
- [13] S. Sathish, V. Anandakrishnan, and M. Gupta, "Optimization of tribological behaviour of magnesium metal-metal composite using pattern search and simulated annealing techniques," *Materials Today Proceedings*, vol. 21, pp. 492–496, Jul. 2019, doi: [10.1016/j.matpr.2019.06.643](https://doi.org/10.1016/j.matpr.2019.06.643).
- [14] A. Namdev, A. Telang, R. Purohit, R. Malviya, and R. S. Rana, "Tribological and mechanical behaviour of alumina particles reinforced LM24 alloy," *Materials Today Proceedings*, vol. 26, pp. 3167–3172, Jan. 2020, doi: [10.1016/j.matpr.2020.02.653](https://doi.org/10.1016/j.matpr.2020.02.653).
- [15] S. T. Reddy, H. S. Manohar, and S. N. Anand, "Effect of carbon black nano-fillers on tribological properties of Al6061-Aluminium metal matrix composites," *Materials Today Proceedings*, vol. 20, pp. 202–207, Dec. 2019, doi: [10.1016/j.matpr.2019.11.045](https://doi.org/10.1016/j.matpr.2019.11.045).
- [16] S. N. Alam and L. Kumar, "Mechanical properties of aluminium based metal matrix composites reinforced with graphite nanoplatelets," *Materials Science and Engineering A*, vol. 667, pp. 16–32, Apr. 2016, doi: [10.1016/j.msea.2016.04.054](https://doi.org/10.1016/j.msea.2016.04.054).
- [17] R. K. Uyyuru, M. K. Surappa, and S. Brusethaug, "Tribological behavior of Al–Si–SiCp composites/automobile brake pad system under dry sliding conditions," *Tribology International*, vol. 40, no. 2, pp. 365–373, Sep. 2006, doi: [10.1016/j.triboint.2005.10.012](https://doi.org/10.1016/j.triboint.2005.10.012).
- [18] P. J. Blau and H. M. Meyer, "Characteristics of wear particles produced during friction tests of conventional and unconventional disc brake materials," *Wear*, vol. 255, no. 7–12, pp. 1261–1269, Apr. 2003, doi: [10.1016/s0043-1648\(03\)00111-x](https://doi.org/10.1016/s0043-1648(03)00111-x).
- [19] M. A. E. Chaparro et al., "Urban and suburban's airborne magnetic particles accumulated on Tillandsia capillaris," *The Science of the Total Environment*, vol. 907, p. 167890, Oct. 2023, doi: [10.1016/j.scitotenv.2023.167890](https://doi.org/10.1016/j.scitotenv.2023.167890).
- [20] G. Piras, F. Pini, and P. Di Girolamo, "PM₁₀ emissions from tires: A disruptive estimate questioning present pollution mitigation strategies," *Atmospheric Pollution Research*, vol. 15, no. 1, p. 101939, Oct. 2023, doi: [10.1016/j.apr.2023.101939](https://doi.org/10.1016/j.apr.2023.101939).
- [21] Y. Wang et al., "A new method to assess vehicle airborne non-exhaust particles: Principle, application and emission evaluation," *Applied Energy*, vol. 352, p. 121942, Sep. 2023, doi: [10.1016/j.apenergy.2023.121942](https://doi.org/10.1016/j.apenergy.2023.121942).
- [22] P. Jayashree, V. Matejka, A. Sinha, S. Gialanella, and G. Straffellini, "A comprehensive study on the particulate matter characteristics of a friction material containing blast furnace slags," *Tribology International*, vol. 186, p. 108567, May 2023, doi: [10.1016/j.triboint.2023.108567](https://doi.org/10.1016/j.triboint.2023.108567).
- [23] B. Lopez et al., "Metal contents and size distributions of brake and tire wear particles dispersed in the near-road environment," *The Science of the Total Environment*, vol. 883, p. 163561, Apr. 2023, doi: [10.1016/j.scitotenv.2023.163561](https://doi.org/10.1016/j.scitotenv.2023.163561).
- [24] S. F. I. Abdillah and Y.-F. Wang, "Ambient ultrafine particle (PM_{0.1}): Sources, characteristics, measurements and exposure implications on human health," *Environmental Research*, vol. 218, p. 115061, Dec. 2022, doi: [10.1016/j.envres.2022.115061](https://doi.org/10.1016/j.envres.2022.115061).
- [25] S. K. Verma, V. K. Dwivedi, and S. P. Dwivedi, "An Experimental Investigation on Mechanical and Tribological Properties of Metal Matrix Composites Fabricated with Waste Aluminum,

- SAC, and CDPF via Stir Casting,” *Journal of the Institution of Engineers (India) Series D*, Jan. 2024, doi: [10.1007/s40033-024-00644-5](https://doi.org/10.1007/s40033-024-00644-5).
- [26] A. Singla and Y. Singh, “Nanosize Al₂O₃ reinforcement in Si-rich aluminum MMC for enhanced tribological performance in engine components,” *Proceedings of the Institution of Mechanical Engineers Part E Journal of Process Mechanical Engineering*, vol. 238, no. 1, pp. 180–191, Nov. 2022, doi: [10.1177/09544089221139117](https://doi.org/10.1177/09544089221139117).
- [27] C. S. Ramesh and A. Ahamed, “Friction and wear behaviour of cast Al 6063 based in situ metal matrix composites,” *Wear*, vol. 271, no. 9–10, pp. 1928–1939, Jul. 2011, doi: [10.1016/j.wear.2010.12.048](https://doi.org/10.1016/j.wear.2010.12.048).
- [28] S. H. Dhoria, V. D. P. Rao, and K. V. Subbaiah, “Mechanical and wear behaviour of 6351 Al/Gr/SiC composites fabricated by squeeze casting,” *Materials Today Proceedings*, vol. 18, pp. 2107–2113, Jan. 2019, doi: [10.1016/j.matpr.2019.06.326](https://doi.org/10.1016/j.matpr.2019.06.326).
- [29] A. Baradeswaran and A. E. Perumal, “Study on mechanical and wear properties of Al 7075/Al₂O₃/graphite hybrid composites,” *Composites Part B Engineering*, vol. 56, pp. 464–471, Aug. 2013, doi: [10.1016/j.compositesb.2013.08.013](https://doi.org/10.1016/j.compositesb.2013.08.013).
- [30] P. K. Sonker, T. J. Singh, and N. P. Yadav, “Experimental research and effect on mechanical and wear properties of aluminium based composites reinforced with Zn/SiC particles,” *Discover Materials*, vol. 3, no. 1, May 2023, doi: [10.1007/s43939-023-00045-7](https://doi.org/10.1007/s43939-023-00045-7).
- [31] S. C. S. K. A. V. and S. S., “Tribological behavior of AA7075-TiC composites by powder metallurgy,” *Industrial Lubrication and Tribology*, vol. 70, no. 6, pp. 1066–1071, Jul. 2018, doi: [10.1108/ilt-10-2017-0312](https://doi.org/10.1108/ilt-10-2017-0312).
- [32] M. R. Papabathina et al., “Effect of graphite on mechanical and tribological properties of AL6061/SiC hybrid composites,” *Annales De Chimie Science Des Matériaux*, vol. 47, no. 3, pp. 125–132, Jun. 2023, doi: [10.18280/acsm.470301](https://doi.org/10.18280/acsm.470301).
- [33] P. Singh, R. K. Mishra, B. Singh, and V. Gupta, “Mechanical and tribological properties of zinc-aluminium (ZA-27) metal matrix composites: a review,” *Advances in Materials and Processing Technologies*, pp. 1–19, Jan. 2024, doi: [10.1080/2374068x.2024.2304394](https://doi.org/10.1080/2374068x.2024.2304394).
- [34] K. K. Alaneme and P. A. Olubambi, “Corrosion and wear behaviour of rice husk ash—Alumina reinforced Al–Mg–Si alloy matrix hybrid composites,” *Journal of Materials Research and Technology*, vol. 2, no. 2, pp. 188–194, Apr. 2013, doi: [10.1016/j.jmrt.2013.02.005](https://doi.org/10.1016/j.jmrt.2013.02.005).
- [35] S. Ansari, S. Arif, A. H. Ansari, A. Samad, H. Hadidi, and M. Muaz, “Electric resistance sintering of AL-TiO₂-GR hybrid composites and its characterization,” *Sustainability*, vol. 14, no. 20, p. 12980, Oct. 2022, doi: [10.3390/su142012980](https://doi.org/10.3390/su142012980).
- [36] S. Arif, M. T. Alam, A. H. Ansari, M. A. Siddiqui, and M. Mohsin, “Study of mechanical and tribological behaviour of Al/SiC/ZrO₂ hybrid composites fabricated through powder metallurgy technique,” *Materials Research Express*, vol. 4, no. 7, p. 076511, Jul. 2017, doi: [10.1088/2053-1591/aa7b5f](https://doi.org/10.1088/2053-1591/aa7b5f).
- [37] C. A. V. Kumar and J. S. Rajadurai, “Influence of rutile (TiO₂) content on wear and microhardness characteristics of aluminium-based hybrid composites synthesized by powder metallurgy,” *Transactions of Nonferrous Metals Society of China*, vol. 26, no. 1, pp. 63–73, Jan. 2016, doi: [10.1016/s1003-6326\(16\)64089-x](https://doi.org/10.1016/s1003-6326(16)64089-x).
- [38] M. S. Safavi, A. Azarniya, M. F. Ahmadipour, and M. V. Reddy, “New-emerging approach for fabrication of near net shape aluminum matrix composites/nanocomposites: Ultrasonic additive manufacturing,” *Journal of Ultrafine Grained and Nanostructured Materials*, vol. 52, no. 2, pp. 188–196, Dec. 2019, doi: [10.22059/jufgmsm.2019.02.07](https://doi.org/10.22059/jufgmsm.2019.02.07).
- [39] 39-G. Marami, S. M. Saman, and M. A. S. Sadigh, “Enhanced mechanical properties of pure aluminium: Experimental investigation of effects of different parameters,” *Journal of Central South University*, vol. 25, no. 3, pp. 561–569, Mar. 2018, doi: [10.1007/s11771-018-3761-4](https://doi.org/10.1007/s11771-018-3761-4).
- [40] M. S. Ashok Kumar, “Microstructural evaluation of AL-AL₂O₃ composites processed by stir casting technique,” *Journal of Materials and Engineering*, vol. 2, no. 4, pp. 267–272, Oct. 2024, doi: [10.61552/jme.2024.04.004](https://doi.org/10.61552/jme.2024.04.004).
- [41] K. S. K. Reddy, B. R. C. Lekha, K. U. Sakshi, M. S. Chouhan, R. Karthikeyan, and S. Aparna, “Effect of different reinforcements on aluminium composite properties – a review,” *Materials Today Proceedings*, vol. 62, pp. 3963–3967, Jan. 2022, doi: [10.1016/j.matpr.2022.04.572](https://doi.org/10.1016/j.matpr.2022.04.572).
- [42] M. Ravikumar, H. N. Reddappa, and R. Suresh, “Aluminium composites fabrication Technique and Effect of Improvement in their mechanical Properties – a review,” *Materials Today Proceedings*, vol. 5, no. 11, pp. 23796–23805, Jan. 2018, doi: [10.1016/j.matpr.2018.10.171](https://doi.org/10.1016/j.matpr.2018.10.171).
- [43] P. Paramasivam and S. Vijayakumar, “Mechanical characterization of aluminium alloy 6063 using destructive and non-destructive testing,” *Materials Today Proceedings*, vol. 81, pp. 965–968, May 2021, doi: [10.1016/j.matpr.2021.04.312](https://doi.org/10.1016/j.matpr.2021.04.312).